Influence of hydration on the optical properties of 2,2-difluoro-4-methylnaphtho-[1,2-*e*]-1,3,2-dioxaborine. Quantum chemical modeling and experimental study

E. V. Fedorenko,[a] I. B. L´vov,[b] V. I. Vovna,[b] D. Kh. Shlyk,[a] and A. G. Mirochnik[a]*

[a]*Institute of Chemistry of the Far-Eastern Branch of the Russian Academy of Sciences, 159 prosp. 100-letiya Vladivostoka, 690022 Vladivostok, Russian Federation. Fax: +7 (423 2) 31 1889. E-mail: gev@ich.dvo.ru*
[b]*Far Eastern Federal University, 8 ul. Sukhanova, 690000 Vladivostok, Russian Federation*

The influence of hydration on the spectral-luminescence properties of 2,2-difluoro-4-methylnaphtho-[1,2-*e*]-1,3,2-dioxaborine in organic solvents was investigated. The hydration of luminophore molecules was found to cause changes in the luminescence spectrum and bleaching of the solutions. The quantum chemical modeling of the electronic structure and absorption spectra of the compound under study and its hydrated complex was performed by the density functional theory (DFT) with the use of the B3LYP5 functional. The results of calculations confirmed the experimentally observed features.

Key words: quantum chemical modeling, density functional theory (DFT), B3LYP5 functional, β-boron difluoride β-diketonates, luminescence, hydrogen bond, absorption spectra.

Boron difluoride β-diketonates exhibit intense fluorescence both in the crystalline state[1] and in solution.[2—4] Hence, these compounds are promising luminescent dyes for polymers.[5,6] Boron difluoride β-diketonates are used as laser dyes,[7] active components of solar collectors,[8] as well as in organic light-emitting diodes.[9]

We have found for the first time the reversible on-off switching of luminescence upon addition of water to solutions of 2,2-difluoro-4-methylnaphtho-[2,1-*e*]-1,3,2-dioxaborine in organic solvents.[10] Experimental studies and quantum chemical calculations showed that the hydration in aprotic solvents is accompanied by the reorganization of the solvation shell of the luminophore, the formation of hydrogen bonds with water molecules, and the decomposition of the electron-donor-acceptor (EDA) complex, resulting in a sharp change in the spectral-luminescence properties of 2,2-difluoro-4-methylnaphtho-[2,1-*e*]-1,3,2-dioxaborine.

In the present study, we investigated the hydration of 2,2-difluoro-4-methylnaphtho-[1,2-*e*]-1,3,2-dioxaborine (**1**) isomeric to 2,2-difluoro-4-methylnaphtho-[2,1-*e*]-1,3,2-dioxaborine (**2**) in acetone. In our previous studies,[11,12] it has been shown that the geometry of isomer **1** differs from that of **2** (molecule **2** is planar and is highly prone to aggregation in solution, whereas molecule **1** is bent along the line connecting the boron atom and the central carbon atom of the chelate ring and can form only dimers).

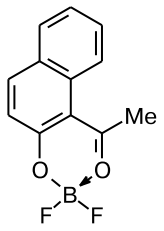

1

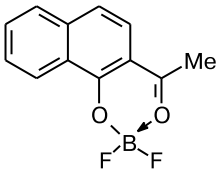

2

The aims of the present study were to investigate the mechanism of the influence of water on the optical properties of isomer **1** in organic solvents by luminescence and quantum chemical methods, to determine the electronic structures of this isomer and its hydrated forms, and to perform the theoretical simulation of the electronic absorption spectra of these compounds.

Experimental

2,2-Difluoro-4-methylnaphtho-[1,2-*e*]-1,3,2-dioxaborine (**1**) was synthesized and purified according to a procedure described in the study.[13] Acetone was dehydrated according to a known procedure.[14]

The luminescence and luminescence excitation spectra were recorded on a Shimadzu RF-5301PC spectrometer. To determine the dynamics of the change in the luminescence spectrum of compound **1** in the course of the hydration, water (0.01 mL) was added to a solution of **1** (4 mL) in anhydrous acetone

Published in Russian in *Izvestiya Akademii Nauk. Seriya Khimicheskaya,* No. 8, pp. 1513—1520, August, 2011.

($C = 10^{-3}$ mol L^{-1}) in a cell equipped with a micro stirrer. To measure the dependence of the luminescence spectrum of this solution on the water concentration, the necessary amounts of a solution of compound **1** with $C = 5 \cdot 10^{-3}$ mol L^{-1} and a solution of water with $C = 10$ mol L^{-1} in anhydrous acetone were diluted to the mark with anhydrous acetone. After stirring, the solutions were stored for 10 min.

Electronic absorption spectra were recorded on a SF-256 spectrophotometer. Time-resolved luminescence spectra were measured on a FluoTime 200 picosecond laser spectrofluorometer (PicoQuant).

Quantum chemical modeling. Quantum chemical calculations were carried out by the density functional theory (DFT).[15] This theory is successfully used for the modeling of the ground state of molecules, and its version based on the time-dependent Kohn—Sham equation (TDDFT)[16] is efficient in calculations of the energies of excited states. The calculations were carried out with the use of the Firefly quantum chemistry package (version 7.1. G)[17] with the 6-31G** basis set using the B3LYP5 exchange-correlation functional.[18]

When modeling the hydration of compound **1**, the energetically most favorable localization site of one water molecule was searched for. To speed up the calculations, this procedure was performed in two steps. In the first step, 23 starting models with different positions and orientations of water molecules around the substrate molecule were constructed. The full geometry optimization was performed by the semiempirical AM1 method,[19] whose reliability of the prediction of the geometric and electronic structures for hydrogen-bonded systems is comparable with *ab initio* methods.

In the first step, two structures with the lowest total energy were obtained. The further geometry optimization of these structures was performed in the second step by the DFT method with the 6-31G** basis set. The results of quantum chemical calculations of the hydrated structure given below correspond to the minimum energy.

The fact that the optimized structure corresponds to a local minimum on the potential energy surface was confirmed by the calculation of the Hessian.

Results and Discussion

After the addition of water to a solution of compound **1** in acetone ($C = 10^{-3}$ mol L^{-1}), the fluorescence intensity decreases by a factor of two and the luminescence maximum is shifted from 450 to 470 nm already in the first minute; the equilibrium is finally established in the system in 6 min (Fig. 1).

The sequential increase in the water concentration (0—0.62 mol L^{-1}) is accompanied by considerable changes in the luminescence spectrum (Fig. 2). An increase in the water concentration from 0 to 0.25 mol L^{-1} leads to sharp luminescence quenching of compound **1** and a bathochromic shift of the band maximum by 20 nm (curves *1*—*3*, see Fig. 2). After the increase in the water concentration to 0.5 mol L^{-1}, the luminescence spectrum shows bands at 405 and 430 nm (curve *4*, see Fig. 2). At $C(H_2O)$ = 0.62 mol L^{-1}, the band at 470 nm disappears and the luminescence intensity increases (curve *5*, see Fig. 2). The

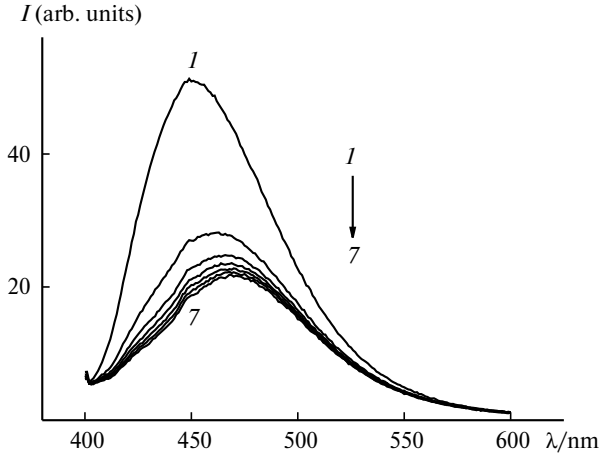

Fig. 1. Changes with time in the luminescence spectrum of a solution of compound **1** ($C = 10^{-3}$ mol L^{-1}) in acetone after the addition of water (0.01 mL) : 0 (*1*) → 6 min (*7*).

fact that the successive increase in the water concentration first leads to a bathochromic shift of the spectrum and luminescence quenching followed by a hypsochromic shift of the spectrum and luminescence enhancement suggests the two-step mechanism of the hydration of luminophore **1**.

To reveal the nature of luminescence centers in the starting solution of compound **1** in anhydrous acetone ($C = 10^{-3}$ mol L^{-1}), we studied the dependence of the spectral-luminescence properties on the concentration of this compound (Fig. 3). When changing from $C = 10^{-3}$ mol L^{-1} to $C = 10^{-4}$ mol L^{-1}, the bands at 401, 409, and 423 nm assigned to monomer luminescence appear in addition to the luminescence band with a maximum at 450 nm.[12] A further dilution of the solution to $C = 10^{-5}$ mol L^{-1} leads to the disappearance of the long-wavelength luminescence band with a maximum at 450 nm.

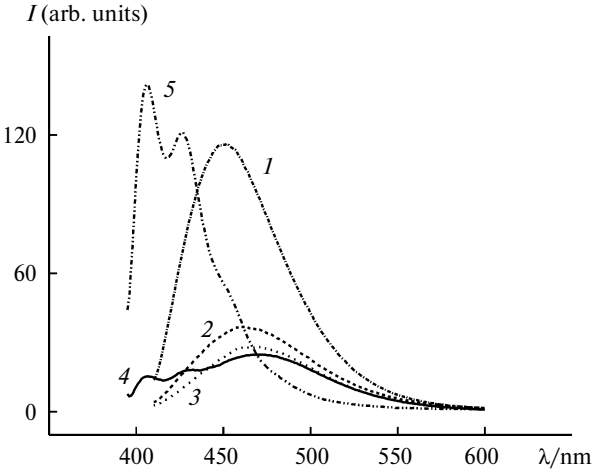

Fig. 2. Dependences the luminescence spectrum of a solution of compound **1** ($C = 10^{-3}$ mol L^{-1}) in acetone on the water concentration, mol L^{-1}: 0 (*1*), 0.12 (*2*), 0.25 (*3*), 0.5 (*4*), 0.62 (*5*).

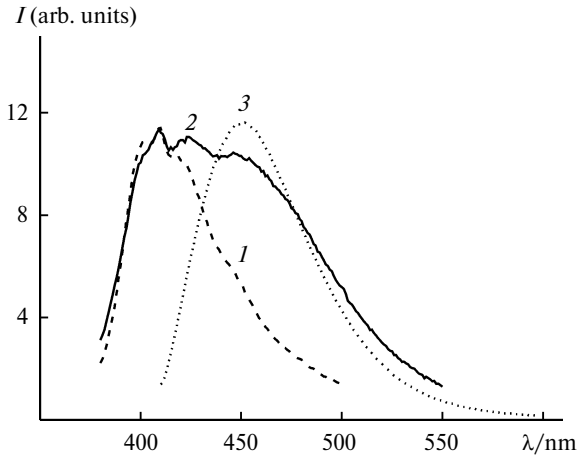

Fig. 3. Dependences of the luminescence spectrum on the concentration of compound **1**, mol L^{-1}: 10^{-5} (*1*), 10^{-4} (*2*), 10^{-3} (*3*).

A broad structureless luminescence band of the starting solution of luminophore **1** ($C = 10^{-3}$ mol L^{-1}) with a maximum at 450 nm, whose intensity in the luminescence spectrum decreases with decreasing concentration of solutions, has an excimer nature.[20] For ground-state molecule **1**, whose chelate ring is puckered, the excimers can have only the dimeric structure similar to the structure of the dimers in the crystal.[11]

The mechanism of the formation of an excimer through the formation of the EDA complex proposed in the study[10] takes place for isomer **1** as well. This is evidenced by the presence of a band at 390 nm in the absorption spectrum of a concentrated solution in acetone and the absence of this band in the spectrum of a dilute solution (Fig. 4, spectra *1* and *2*). This behavior of the absorption spectrum is characteristic of the formation of EDA complexes in the ground state.[21] The simultaneous existence of monomers and dimers of ground-state compound **1** in solution is confirmed by the dependence of the luminescence excitation spectra on the luminescence wavelength of a solution with $C = 10^{-4}$ mol L^{-1} exhibiting both monomer and excimer luminescence (Fig. 5).

The luminescence excitation spectrum of the single molecules (luminescence at 390 and 400 nm) shows bands with maxima at 350, 360, and 365 nm (see Fig. 5, curves *1* and *2*). At wavelengths of excimer luminescence (450 nm and higher), the luminescence excitation spectrum shows only a band at 384 nm (see Fig. 5, curves *4*—*6*) corresponding to the band of the EDA complex in the absorption spectrum (see Figs 4 and 5). In our previous study,[10] we have considered the mechanism of the formation of excimers (excited dimers) through EDA complexes.

Therefore, in a solution of luminophore **1** with $C = 10^{-3}$ mol L^{-1}, the molecules form EDA dimers. The first hydration step of luminophore **1** accompanied by a bathochromic shift of the luminescence spectrum (see Fig. 2) corresponds to the insertion of a water molecule into the solvation shell of the dimer. A hypsochromic shift of the luminescence spectrum at high water concentrations is indicative of the decomposition of the EDA complex between molecules of luminophore **1** and the formation of a new hydrated complex between molecule **1** and a water molecule, which is confirmed by the disappearance of the absorption band at 390 nm upon addition of water (see Fig. 4) and the presence of an inflection point in the Stern—Volmer plot (Fig. 6). This plot indicates that the first hydration step is diffusion-controlled, and the second step affords a stable complex of luminophore **1** with a quencher.

Two luminescence centers in a solution of compound **1** with a water content of 0.5 mol L^{-1}, which displays luminescence of both hydrated dimers and monomers, are

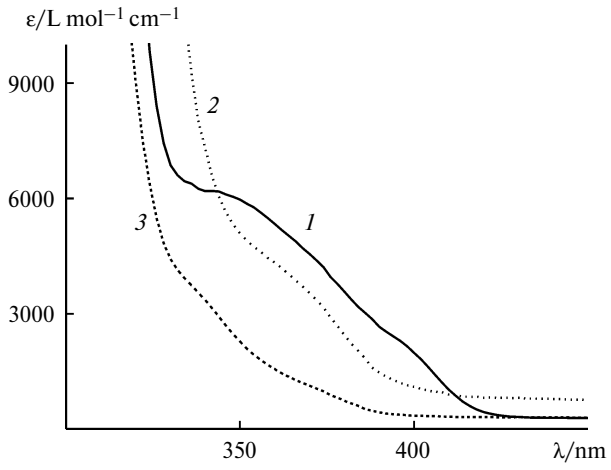

Fig. 4. Absorption spectra of solutions of compound **1** in acetone at C(M) = 0.012 (*1*) and 0.0012 (*2*) and in a 9 : 1 acetone—water mixture at C(M) = 0.012 (*3*).

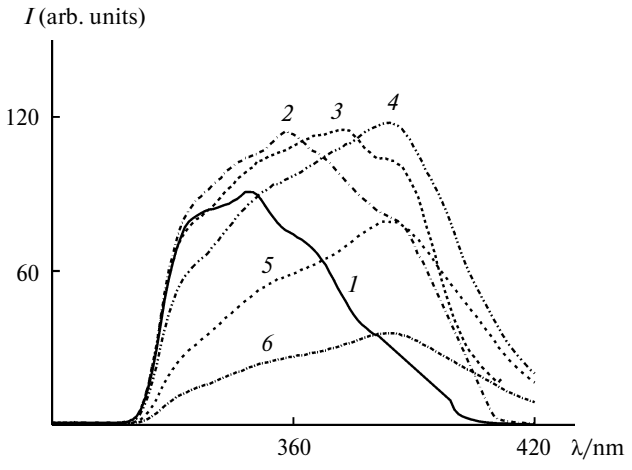

Fig. 5. Dependences of the excitation spectrum on the luminescence wavelength of a solution of compound **1** ($C = 10^{-4}$ mol L^{-1}) in anhydrous acetone (λ_{lum}/nm): 390 (*1*), 400 (*2*), 420 (*3*), 450 (*4*), 490 (*5*), 520 (*6*).

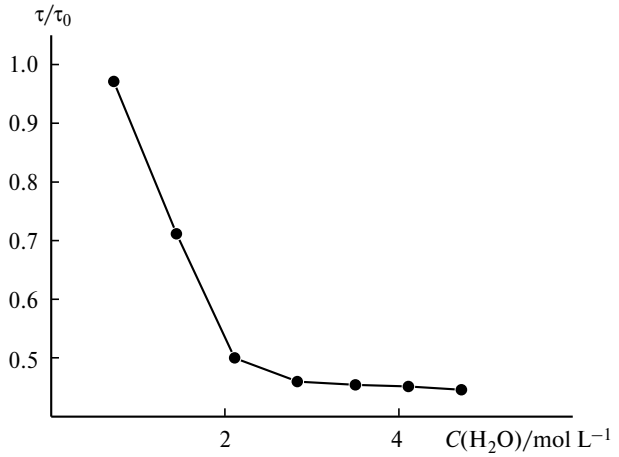

Fig. 6. Stern—Volmer plot for luminescence quenching of a solution of compound **1** ($C = 0.012$ mol L^{-1}) with water.

reliably detected in the time-resolved luminescence spectra (Fig. 7). A decrease with time in the luminescence intensity in the short-wavelength region of the spectrum is indicative of the simultaneous excitation of two luminescence centers and quenching of the short-lived process.

The formation of a stable complex between luminophore **1** and water in the second hydration step was confirmed by investigation of the hydration in a dilute solution displaying luminescence of only single molecules.

For a solution of compound **1** with a concentration of 10^{-5} mol L^{-1}, the addition of water leads to changes in the luminescence and luminescence excitation spectra, which is evidence of the formation of a complex between water and the luminophore in the ground state (Fig. 8). In the luminescence excitation spectrum, the band at 367 nm is shifted to 374 nm. In the luminescence spectrum, the band at 405 nm is observed instead of the bands at 400 and

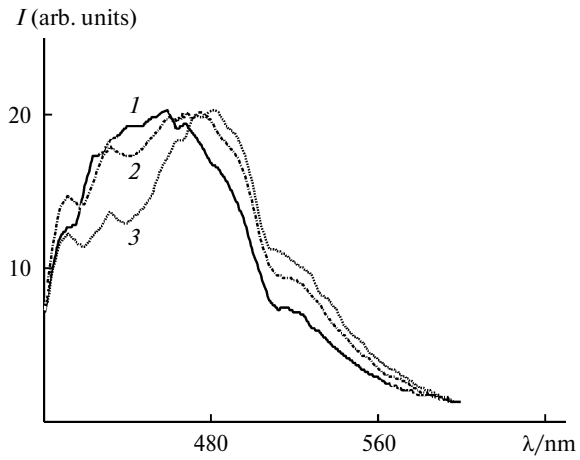

Fig. 7. Time-resolved spectra of a solution of compound **1** ($C = 10^{-3}$ mol L^{-1}) in acetone at a water concentration of 0.5 mol L^{-1}. The period of time after the instant of excitation of the system, ns: 0 (*1*), 0.7 (*2*), 2.1 (*3*).

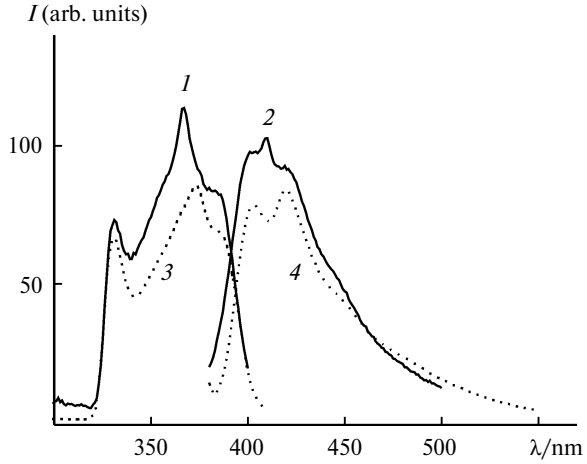

Fig. 8. Luminescence and luminescence excitation spectra of solutions of compound **1** ($C = 10^{-5}$ mol L^{-1}) in anhydrous acetone (*1*, *2*) and acetone with $C(H_2O) = 0.5$ mol L^{-1} (*3*, *4*).

410 nm. This spectrum of hydrated single molecules is observed in a solution with a luminophore concentration of 10^{-3} mol L^{-1} and a water concentration of 0.62 mol L^{-1} (curve 5, see Fig. 2).

To elucidate the mechanism of the observed phenomena, we performed quantum chemical calculations of structure **1** and its hydrated forms. Figure 9 shows the hydrated structure of 2,2-difluoro-4-methylnaphtho-[1,2-*e*]-1,3,2-dioxaborine (**1´**) corresponding to the energy minimum. The geometric parameters of structures **1** and **1´** calculated by the DFT method are given in Table 1, which also presents the experimental interatomic distances and bond angles.[11] A comparison of the results of the quantum chemical modeling of isolated molecule **1** with the X-ray diffraction data for the crystalline system is indica-

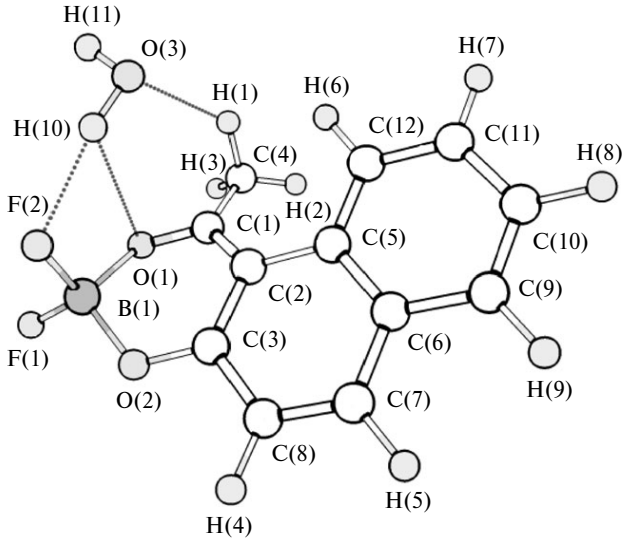

Fig. 9. Arrangement of the water molecule with respect to the substrate according to the calculated data (structure **1´**).

Table 1. Geometric parameters of structures **1** and **1´**

Parameter*	Structure **1**		Structure **1´**
	Calculation	Experiment	Calculation
Bond		*d*/Å	
B(1)—F(1)	1.356	1.355/1.352	1.353
B(1)—F(2)	1.369	1.376/1.381	1.396
B(1)—O(1)	1.539	1.502/1.510	1.523
B(1)—O(2)	1.493	1.457/1.459	1.483
O(1)—C(1)	1.284	1.282/1.293	1.288
O(2)—C(3)	1.305	1.321/1.329	1.381
C(1)—C(2)	1.425	1.417/1.424	1.425
C(2)—C(3)	1.429	1.411/1.408	1.426
C(1)—C(4)	1.503	1.499/1.478	1.498
H(10)—F(2)	—	—	1.931
H(1)—O(3)	—	—	2.467
H(10)—O(1)	—	—	2.756
Bond angle		ω/deg	
F(1)—B(1)—F(2)	115.4	111.6/111.1	113.9
O(1)—B(1)—O(2)	105.4	108.4/108.6	106.1
Dihedral angle		φ/deg	
B(1)—O(2)—C(3)—C(2)	15.9	—	15.2
B(1)—O(1)—C(1)—C(4)	175.1	—	171.8

* The corresponding values for both molecules in the dimer are given.

tive of a good agreement between the calculated and experimental geometry.

The H(10)—O(1) interatomic distance suggests that one of the hydrogen atoms of the water molecule forms hydrogen bonds not only with the fluorine atom but also with the oxygen atom of luminophore **1**. The spatial localization of the water molecule is also favorable for the formation of the six-membered cyclic structure O(1)—C(1)—C(4)—H(1)—O(3)—H(10). According to the calculations, the gain in the energy upon the formation of compound **1´** from noninteracting water and substrate molecules is 0.44 eV.

The orbital structures of compounds **1** and **1´** are presented in Table 2. In both structures, the π-type molecular orbitals delocalized over the molecules are the highest occupied MO. The lowest unoccupied molecular orbitals of both structures are also π-type orbitals. Figure 10 shows HOMO and LUMO of luminophore **1**. These orbitals in compound **1´** are characterized by a similar electron density distribution. According to the calculations, the energies of the molecular orbitals with a considerable contribution from AO of the fluorine atoms vary from –9 to –10 eV. The n_--MO is pronounced, whereas the n_+-MO is strongly mixed with σ-MO, which is characteristic of this class of compounds.* According to the calculations, the energy of the π→π transition from HOMO to LUMO is 3.87 eV for both structures.

To determine the parameters of the electron transitions and elucidate the influence of a water molecule on these transitions, the electronic absorption spectra of structures **1** and **1´** were calculated by the TDDFT method. The oscillator forces and the energies of the transitions corresponding to twenty excited states of structures **1** and **1´** are given in Tables 3 and 4, respectively.

The first two long-wavelength bands in the calculated electronic absorption spectra of structures **1** and **1´** have the same nature and correspond to the virtually pure one-electron π→π transitions (Fig. 11). Most of the other bands correspond to the excited states formed as a result of multielectron transitions. Thus, the most intense band at 209 nm

* The *n* orbitals correspond to the oxygen lone pairs; the signs of two *p* orbitals of the oxygen atoms in the chelate ring are either the same (n_+) or opposite (n_-).

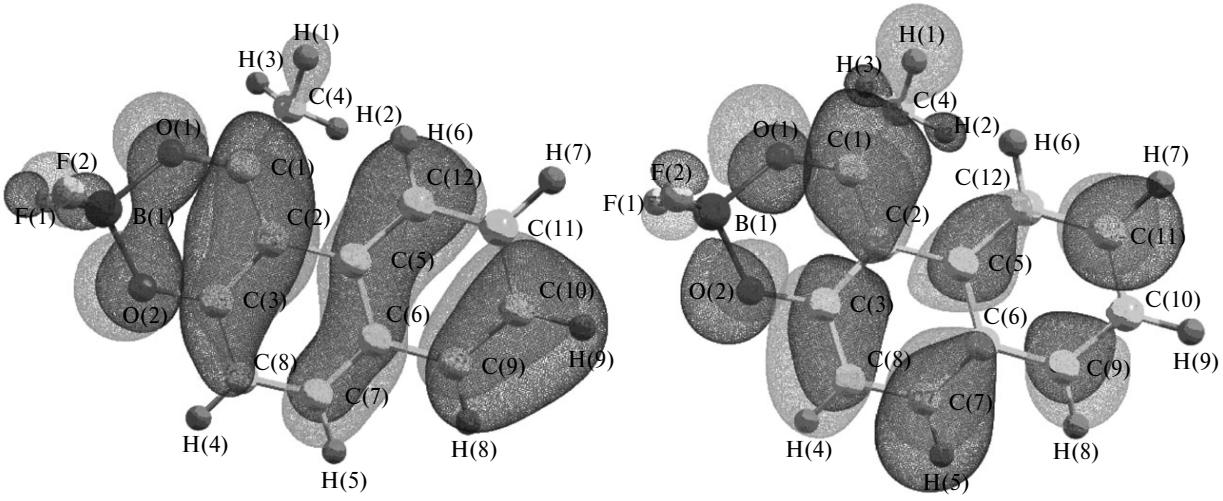

Fig. 10. Molecular orbitals of structure **1**: HOMO (*a*), LUMO (*b*).

Table 2. Energies E and compositions of the molecular orbitals of structures **1** and **1´**

N^a	Type	Composition[b] (%)	E/eV
		Structure **1**	
64[c]	π	$C_\kappa(57) + C_\gamma(13)$	0.62
63[c]	π	$C_\kappa(73) + C_\beta(19)$	−0.57
62[c]	π	$C_\kappa(72) + C_\beta(16)$	−0.98
61[c]	π	$C_\kappa(37) + C_\beta(36) + O(19)$	−2.59
60	π	$C_\kappa(50) + C_\gamma(19) + O(16) + C_\beta(11)$	−6.46
59	π	$C_\kappa(90)$	−6.85
58	π	$C_\kappa(49) + O(21) + C_\gamma(19)$	−8.18
57	*n*	$O(45) + C_\kappa(24) + C_\gamma(10)$	−8.39
56	π	$C_\kappa(68) + F(16) + O(14)$	−8.76
55	π	F(84)	−9.18
54	π	$F(75) + C_\kappa(12)$	−9.46
53	σ	$F(46) + O(22) + C_\kappa(13)$	−9.62
52	σ	$C_\kappa(49) + F(13)$	−9.76
51	σ	$F(42) + C_\kappa(31)$	−9.89
50	σ	$C_\kappa(35) + F(30) + O(15)$	−10.03

N	Type	Composition (%)	E/eV
		Structure **1´**	
69[c]	π	$C_\kappa(57) + C_\gamma(13) + C_\beta(10)$	0.68
68[c]	π	$C_\kappa(73) + C_\beta(20)$	−0.50
67[c]	π	$C_\kappa(70) + C_\beta(17)$	−0.86
66[c]	π	$C_\kappa(37) + C_\beta(36) + O(18)$	−2.54
65	π	$C_\kappa(54) + C_\gamma(19) + O(14) + C_\beta(11)$	−6.41
64	π	$C_\kappa(89)$	−6.78
63	H_2O	$H_2O(95)$	−7.45
62	π	$C_\kappa(57) + C_\gamma(22) + O(14)$	−8.11
61	*n*	$O(47) + C_\kappa(22)$	−8.44
60	π	$C_\kappa(70) + O(18)$	−8.76
59	σ	$F(73) + H_2O(16)$	−9.42
58	σ	$F(47) + C_\kappa(23)$	−9.64
57	σ	$C_\kappa(38) + F(29)$	−9.67
56	σ	$C_\kappa(38) + O(19) + F(18)$	−9.72
55	σ	$H_2O(58) + F(17)$	−9.93
54	σ	$F(39) + C_\kappa(31) + O(12)$	−10.02
53	σ	$F(48) + O(24)$	−10.09

[a] N is the number of the occupied molecular orbital.
[b] C_κ is the sum of contributions from AO of the C(5)—C(12) atoms of the aromatic rings; C_β and C_γ are the sums of contributions from AO of the C(2) and C(1) + C(3) atoms, respectively; O and F are the sums of contributions from AO of the oxygen and fluorine atoms, respectively; H_2O is the sum of contributions from AO of the oxygen and hydrogen atoms of the water molecule. The contributions smaller than 10% are not given.
[c] Unoccupied orbitals.

Table 3. Energies (ΔE) and oscillator forces (f) of singlet-singlet transitions in the electronic absorption spectrum of structure **1** calculated at the B3LYP5/6-31G** level of theory

State	ΔE/eV	ΔE/cm^{-1}	ΔE/nm	f	Transition*
1	3.48	28074	356.21	0.09	60→61 (96)
2	3.74	30177	331.38	0.12	59→61 (93)
3	4.54	36625	273.04	0.00	57→61 (56) + 58→61 (40)
4	4.84	39071	255.94	0.05	60→62 (51) + 60→63 (22) + 59→62 (17)
5	4.95	39961	250.24	0.03	58→61 (47) + 57→61 (32) + 60→62 (9)
6	5.20	41941	238.43	0.11	59→62 (31) + 60→62 (29) + 60→63 (21) + 58→61 (8)
7	5.31	44470	224.87	0.00	56→61 (68) + 59→63 (17)
8	5.75	46400	215.52	0.15	55→61 (63) + 60→63 (14) + 59→62 (10)
9	5.94	47904	208.75	0.58	60→63 (27) + 59→62 (25) + 55→61 (25)
10	5.97	48168	207.61	0.00	53→61 (66) + 54→61 (15)
11	6.07	48937	204.34	0.09	59→63 (43) + 54→61 (18) + 56→61 (11) + 58→62 (10)
12	6.18	49836	200.66	0.02	54→61 (53) + 53→61 (16) + 52→61 (15)
13	6.25	50376	198.51	0.01	52→61 (71) + 54→61 (8)
14	6.31	50854	196.64	0.08	60→64 (74) + 58→62 (13)
15	6.39	51575	193.89	0.00	51→61 (80) + 50→61 (11)
16	6.52	52562	190.25	0.05	57→62 (49) + 58→62 (15) + 50→61 (15) + 53→61 (9)
17	6.62	53419	187.20	0.00	50→61 (64) + 57→62 (16) + 51→61 (12)
18	6.65	53624	186.48	0.05	59→64 (51) + 58→63 (25)
19	6.82	54993	181.84	0.01	57→63 (54) + 58→63 (31)
20	6.95	56049	178.42	0.24	58→62 (33) + 59→64 (20) + 57→62 (13) + 56→62 (9)

* The numbers of the molecular orbitals correspond to those given in Table 2. The contributions from transitions in percentage are given in parentheses. The contributions smaller than 8% are not given.

Table 4. Energies (ΔE) and oscillator forces (f) of singlet-singlet transitions in the electronic absorption spectrum of structure **1´** calculated at the B3LYP5/6-31G** level of theory

State	ΔE/eV	ΔE/cm^{-1}	ΔE/nm	f	Transition*
1	3.46	27927	358.08	0.10	65→66 (96)
2	3.72	29973	333.64	0.11	64→66 (94)
3	4.47	36056	277.35	0.01	63→66 (94)
4	4.69	37824	264.38	0.01	61→66 (59) + 62→66 (31)
5	4.89	39447	253.50	0.04	65→67 (38) + 65→68 (27) + 64→67 (24)
6	4.96	39994	250.04	0.04	62→66 (54) + 61→66 (25) + 65→67 (11)
7	5.21	42018	237.99	0.12	65→67 (41) + 64→67 (26) + 65→68 (17)
8	5.55	44761	223.41	0.00	60→66 (64) + 64→68 (20)
9	5.91	47633	209.94	0.59	65→68 (36) + 64→67 (34)
10	6.06	48871	204.62	0.14	56→66 (28) + 59→66 (21) + 64→68 (14)
11	6.12	49325	202.74	0.05	59→66 (37) + 64→68 (23) + 57→66 (12)
12	6.13	49461	202.18	0.03	59→66 (27) + 56→66 (26) + 58→66 (20) + 64→68 (14)
13	6.21	50109	199.56	0.02	63→67 (64) + 57→66 (17)
14	6.23	50287	198.86	0.02	57→66 (34) + 63→67 (30) + 58→66 (11)
15	6.30	50851	196.56	0.06	65→69 (73) + 62→67 (16)
16	6.40	51606	193.77	0.00	58→66 (44) + 57→66 (33) + 56→66 (18)
17	6.51	52474	190.57	0.00	54→66 (56) + 55→66 (18)
18	6.61	53292	187.64	0.03	64→69 (30) + 62→68 (19) + 54→66 (16) + 63→68 (14)
19	6.64	53577	186.56	0.00	55→66 (40) + 54→66 (20) + 64→69 (13)
20	6.66	53683	186.28	0.00	63→68 (80) + 64→69 (10)

* The numbers of the molecular orbitals correspond to those given in Table 2. The contributions from transition in percentage are given in parentheses. The contributions smaller than 10% are not given.

is associated with a series of π→π electron transitions. The n→π and σ→π transitions have low intensity and are almost absent in the spectra. The third low-intensity band (f = 0.01) in the electronic absorption spectrum of compound **1´** corresponds to the charge transfer from the water molecule to the substrate. This is indicative of the direct involvement of the solvent in the electron transitions in the course of excitation, which is reflected in the absorption and luminescence spectra of the structures under consideration.

As can be seen from Fig. 11, a small long-wavelength shift of a series of bands is observed in the electronic ab-

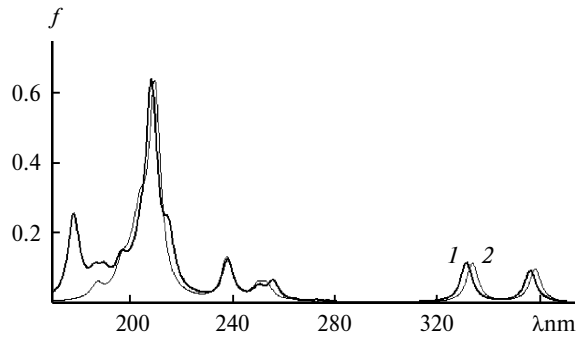

Fig. 11. Electronic absorption spectra of compound **1** (*1*) and hydrated structure **1´** (*2*) calculated by the B3LYP5/6-31G** method.

Table 5. Changes in the electron populations of the X, E, and W groups (see the text) in 20 excited states of structures **1** and **1´**

State	Structure **1**		Structure **1´**	
	Δq_X	Δq_X	Δq_E	Δq_W
1	0.14	0.17	−0.17	0.00
2	0.54	0.54	−0.54	0.00
3	−0.20	0.54	0.33	−0.87
4	−0.07	−0.10	0.20	−0.10
5	0.03	−0.02	0.03	0.00
6	−0.01	0.02	−0.02	0.00
7	0.23	0.00	0.01	−0.01
8	−0.29	0.27	−0.27	0.00
9	−0.21	−0.17	0.18	0.00
10	−0.16	−0.04	0.10	−0.06
11	−0.07	0.14	−0.06	−0.08
12	−0.06	−0.09	0.12	−0.02
13	0.26	0.23	0.39	−0.63
14	−0.03	0.24	0.08	−0.31
15	0.08	−0.03	0.04	−0.01
16	−0.46	−0.12	0.24	−0.12
17	−0.20	0.07	−0.02	−0.05
18	0.25	0.18	0.00	−0.17
19	−0.50	0.13	0.21	−0.33
20	−0.03	0.19	0.60	−0.33

Note. The minus sign indicates a decrease in the electron population.

sorption spectrum of hydrated structure **1´**, which is consistent with the experimental data. Thus, the addition of small amounts of water to compound **1** leads to a bathochromic shift of the bands in the luminescence excitation spectra (see Fig. 8).

To analyze the nature of the spectral bands, the total Mulliken atomic populations in the ground and excited states of structures **1** and **1´** were calculated in the unrelaxed density approximation. Table 5 gives the changes in the populations for individual fragments with respect to the ground state that occur in the course of excitation. According to Fig. 9, the symbol X stands for the chelate moiety consisting of the boron, fluorine, oxygen, and carbon atoms of the chelate ring (C(1)—C(3)) and the methyl group, the symbol E indicates the carbon and hydrogen atoms of the naphthalene moiety (except for the C(2) and C(3) atoms), and the symbol W denotes the oxygen and hydrogen atoms of the water molecule.

The first two bands in the calculated spectra of structures **1** and **1´** reflect the partial electron density transfer from the aromatic moiety to the chelate ring, the transfer assigned to the second band being more pronounced. It is interesting that the water molecule can serve only as an electron density donor for the calculated states of structure **1´** in the course of excitation.

In spite of the fact that for a real solution, it is necessary to take into account a complex combination of intermolecular interactions (aggregation and solvation of luminophore molecules), which have a substantial effect on the photophysical properties of the complexes, the above-considered quantum chemical modeling confirmed the experimentally observed characteristic features of the hydration of compound **1**. This process in aprotic solvents occurs in two steps. It is accompanied by the reorganization of the solvation shell of the luminophore, the formation of hydrogen bonds with water molecules, and the decomposition of the EDA complex, resulting in a sharp change in the spectral characteristics of structure **1**.

References

1. A. G. Mirochnik, E. V. Gukhman, V. E. Karasev, P. A. Zhikhareva, *Izv. Akad. Nauk, Ser. Khim.*, 2000, 1030 [*Russ. Chem. Bull., Int. Ed.*, 2000, **49**, 1024].
2. H.-D. Ilge, D. Fabler, H. Hartman, *Z. Chem.*, 1984, **24**, 218.
3. H.-D. Ilge, H. Hartmann, *Z. Chem.*, 1986, **26**, 399.
4. G. Gorlitz, H. Hartmann, J. Kossanyi, P. Valat, V. Wintgens, *Ber. Bunsenges. Phys. Chem.*, 1998, **102**, 1449.
5. Ger. (East) DD/-265266, 1987, *Chem. Abstrs.*, 1990, **112**, 45278.
6. WO 02/065600, *Chem. Abstrs.*, 2003, **137**, 187010.
7. Ger. (East) DD/-265266, 1987, *Chem. Abstrs*, 1990, **112**, 45278.
8. Ger. Pat. 10152938, *Chem. Abstrs*, 2003, **123**, 378622.
9. WO 02/065600, *Chem. Abstrs*, 2003, **137**, 187010.
10. E. V. Fedorenko, I. B. L´vov, V. I. Vovna, D. Kh. Shlyk, A. G. Mirochnik, *Izv. Akad. Nauk, Ser. Khim.*, 2010, 1017 [*Russ. Chem. Bull., Int. Ed.*, 2010, **59**, 1041].
11. B. V. Bukvetskii, E. V. Fedorenko, A. G. Mirochnik, V. E. Karasev, *Zh. Strukt. Khim.,* 2006, **47**, 60 [*Russ. J. Struct. Chem.* (*Engl. Transl.*), 2006, **47**, 56].
12. E. V. Fedorenko, A. G. Mirochnik, V. E. Karasev, B. V. Bukvetskii, *Zh. Fiz. Khim.*, 2006, **80**, 2192 [*Russ. J. Phys. Chem.* (*Engl. Transl.*), 2006, **80**, 1953].
13. J. A. Van Allan, G. A. Reynolds, *J. Heterocycl. Chem.,* 1969, **6**, 29.
14. A. J. Gordon, R. A. Ford. *The Chemist´s Companion: a Handbook of Practical Data, Techniques and References*, Wiley, New York, 1972.
15. R. G. Parr, W. Yang, *Density-Functional Theory of Atoms and Molecules*, Oxford University Press, New York, 1989.
16. E. Runge, E. K. U. Gross, *Phys. Rev. Lett.*, 1984, **52**, 997.
17. A. A. Granovsky, Firefly version 7.1. G, http://classic. chem. msu. su/gran/firefly/index. html.
18. C. Lee, W. Yang, R. G. Parr, *Phys. Rev. B*, 1988, **37**, 785.
19. M. J. S. Dewar, E. G. Zoebisch, E. F. Healy, J. J. P. Stewart, *J. Am. Chem. Soc.*, 1985, **107**, 3902.
20. N. N. Barashkov, T. V. Sakhno, Z. N. Nurmukhametov, O. A. Khakhel´, *Usp. Khim.*, 1993, **62**, 579 [*Russ. Chem. Rev.* (*Engl. Transl.*), 1993, **62**].
21. E. I. Kapinus, *Fotonika molekulyarnykh kompleksov* [*Photonics of Molecular Complexes*], Naukova dumka, Kiev, 1988, 256 (in Russian).

Received January 24, 2011;
in revised form May 26, 2011